ORIGINAL RESEARCH

Low-Cost Fetal Magnetocardiography: A Comparison of Superconducting Quantum Interference Device and Optically Pumped Magnetometers

Sarah Strand, PhD; William Lutter, PhD; Janette F. Strasburger, MD; Vishal Shah, PhD; Oswaldo Baffa, PhD; Ronald T. Wakai, PhD

***Background*—**Fetal magnetocardiography (fMCG) is a highly effective technique for evaluation of fetuses with life-threatening arrhythmia, but its dissemination has been constrained by the high cost and complexity of Superconducting Quantum Interference Device (SQUID) instrumentation. Optically pumped magnetometers (OPMs) are a promising new technology that can replace SQUIDs for many applications. This study compares the performance of an fMCG system, utilizing OPMs operating in a person-sized magnetic shield, to that of a conventional fMCG system, utilizing SQUID magnetometers operating in a magnetically shielded room.

***Methods and Results*—**fMCG recordings were made in 24 subjects using the SQUID system with the mother lying supine in a magnetically shielded room and the OPM system with the mother lying prone in a person-sized, cylindrical shield. Signal-to-noise ratios of the OPM and SQUID recordings were not statistically different and were adequate for diagnostic purposes with both technologies. Although the environmental noise was higher using the small open-ended shield, this was offset by the higher signal amplitude achieved with prone positioning, which reduced the distance between the fetus and sensors and improved patient comfort. In several subjects, fMCG provided a differential diagnosis that was more precise and/or definitive than was possible with echocardiography alone.

***Conclusions*—**The OPM-based system was portable, improved patient comfort, and performed as well as the SQUID-based system at a small fraction of the cost. Electrophysiological assessment of fetal rhythm is now practical and will have a major impact on management of fetuses with long QT syndrome and other life-threatening arrhythmias. **(*J Am Heart Assoc*. 2019;8:e013436. DOI: 10.1161/JAHA.119.013436.)**

Key Words: magnetocardiography • arrhythmia • electrophysiology • fetal heart • long QT syndrome

Fetal magnetocardiography (fMCG), the magnetic analog of fetal ECG, is an emerging technology that is uniquely suited for investigation of the nascent area of fetal cardiac electrophysiology. Owing to its ability to assess fetal heart rate, rhythm, and conduction with efficacy similar to that of postnatal ECG, it has provided invaluable insight into the mechanisms of fetal arrhythmias and improved the diagnosis and management of this group of diseases.[1–4]

The efficacy of fMCG for clinical evaluation of serious fetal arrhythmia was acknowledged in the recent American Heart Association Statement on Diagnosis and Treatment of Fetal Cardiac Disease.[5]

Despite its advantages, fMCG is not widely utilized. A major barrier to clinical adoption is the high cost and complexity of Superconducting Quantum Interference Device (SQUID) technology.[6] SQUIDs require complex cryogenics, consume large amounts of liquid helium (a scarce natural resource), and must operate within a large, expensive magnetically shielded room (MSR). Until recently, SQUIDs have been the only magnetometers with sufficient sensitivity to record the fMCG. This situation changed, however, following the demonstration of a new type of optically pumped magnetometer (OPM) that can achieve SQUID sensitivity in a room temperature device.[7] In the succeeding years, considerable effort has been devoted to making OPMs small and easy to use. High-performance OPMs that meet

From the Department of Medical Physics, University of Wisconsin, Madison, WI (S.S., W.L., R.T.W.); Division of Cardiology, Department of Pediatrics, Children's Hospital of Wisconsin- Milwaukee, Milwaukee, WI (J.F.S.); QuSpin, Inc., Louisville, CO (V.S.); Department of Physics, FFCLRP, Ribeirao Preto, University of Sao Paulo, Brazil (O.B.).

Correspondence to: Ronald T. Wakai, PhD, Department of Medical Physics, Wisconsin Institutes for Medical Research, 1111 Highland Ave, Madison, WI 53705-2275. E-mail: rtwakai@wisc.edu

Received May 30, 2019; accepted July 15, 2019.

Clinical Perspective

What Is New?

- By combining a new type of biomagnetometer with a person-sized magnetic shield, we have demonstrated a fetal magnetocardiography system that is far more practical and cost-effective than earlier systems.

What Are the Clinical Implications?

- This advance has the potential to greatly increase the utilization of fetal magnetocardiography and enable routine assessment of the cardiac electrophysiology of the fetus.
- The system can be easily reconfigured for other applications, such as adult magnetocardiography.

these criteria are now available. Recently, we performed a head-to-head comparison of OPMs and SQUIDs in an MSR by recording from the same subjects during the same session.[8] The signal-to-noise ratio (SNR) was modestly higher for the SQUID data; however, the signal quality of the OPM data was still sufficiently high to permit accurate diagnosis of fetal arrhythmia.

In this study, we again compare OPM and SQUID fMCG systems, but with the critical difference that the OPM sensors are operated within a person-sized cylindrical shield (CS). Replacement of the MSR by a small, portable shield is essential to the goal of transforming fMCG into a cost-effective clinical technique. The main drawback of person-sized shields is the risk of claustrophobia. We therefore deemed it essential to leave 1 end of the shield open, even though this significantly degraded the shielding performance. This article describes the means by which this problem was compensated and demonstrates the application of the system for rhythm assessment in normal fetuses and fetuses at risk of arrhythmia. The results confirm the excellent technical capabilities of the system and further validate the utility of fMCG as a critical adjunct to ultrasound for evaluation of fetuses with life-threatening arrhythmia, including long QT syndrome (LQTS).

Methods

The data that support the findings of this study are available from the corresponding author upon reasonable request.

fMCG is noninvasive and is believed to be safe. The magnetic sensors are passive recording devices that do not emit magnetic fields or energy. The protocol was approved by the University of Wisconsin Health Sciences Institutional Review Board. Informed consent was obtained from all subjects.

Environment

The study was performed in the Imaging Center of the Wisconsin Institutes for Medical Research, a translational research facility, connected directly to the University of Wisconsin Hospital and Clinics. The magnetic environment is similar to that of a typical hospital with elevators and magnetic resonance scanners located down the hall, ≈25 m away. Power spectra of the environmental magnetic noise are shown in Figure 1.

Subjects

The subjects were 24 healthy women—6 with uncomplicated pregnancies, 2 with high-risk obstetrical conditions, and 16 with pregnancies complicated by fetal arrhythmia or risk of fetal arrhythmia attributed to family history (Table). They were studied at 20 to 35 weeks' gestation (mean, 27.4). Two subjects returned for follow-up sessions; however, to avoid bias, we used data from the session in which the fetal arrhythmia was most prevalent. The women with normal pregnancies were recruited locally; the women with pregnancies complicated by arrhythmia were referred for study by pediatric cardiologists at various centers around the country.

Instrumentation

The fMCG recordings were made using 2 systems: a multichannel SQUID magnetometer (Tristan 624 Biomagnetometer; Tristan Technologies, San Diego, CA) and an array of OPM sensors (QuSpin Zero Field Magnetometer; QuSpin Inc, Louisville, CO).

The Tristan 621/624 is currently the only US Food and Drug Administration–approved fMCG device. It is a 7-channel vector gradiometer, comprised of 21 SQUID sensors, configured to measure 3 orthogonal z-gradient magnetic field components at 7 locations. The 7 channels are arranged in a hexagonal pattern with 4.71-cm channel-to-channel spacing and 8-cm baseline. The magnetic field resolution per channel was 3 to 7 $fT/(Hz)^{1/2}$.

The QuSpin OPMs are stand-alone, single sensors with an outer dimension of $13 \times 19 \times 110$ mm. Each sensor measures 2 orthogonal components of the magnetic field, 1 parallel to the long axis of the sensor and the other parallel to the short axis. The intrinsic magnetic field resolution of the sensors was 10 to 15 $fT/(Hz)^{1/2}$. To optimize the sensitivity of the OPMs, the residual DC magnetic field was nulled to ≈10 nT. This was accomplished by orienting the CS with its long axis perpendicular to the earth's magnetic field and cancelling the residual field by applying small constant currents through a set of triaxial magnetic coils mounted within the CS. The axial coil was in a Helmholtz configuration and the transverse coils were paired

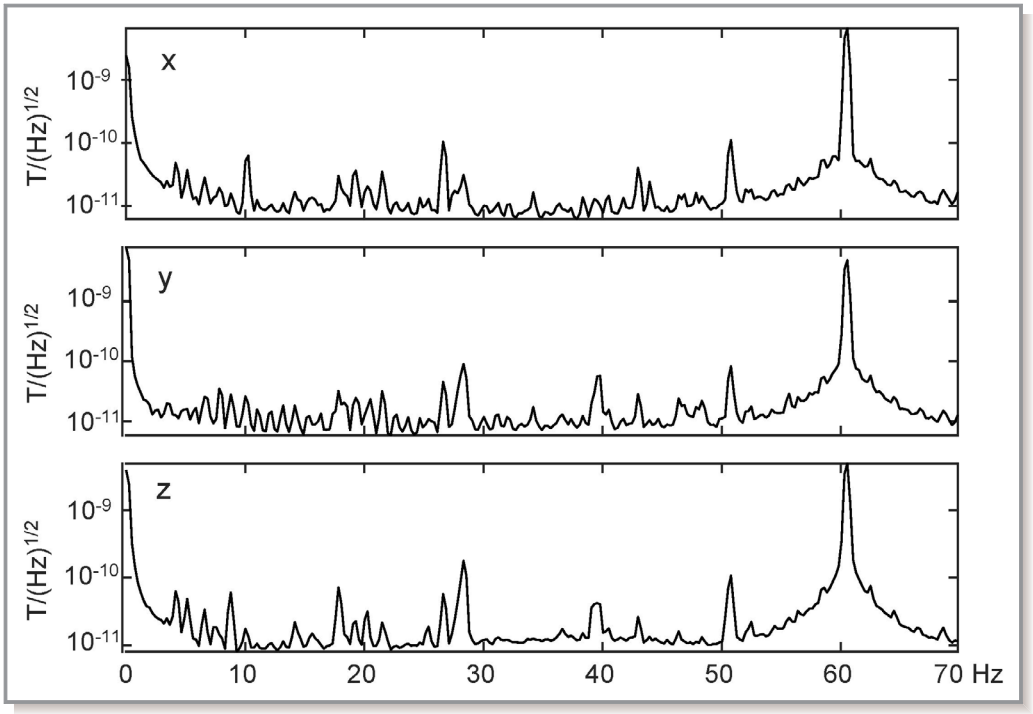

Figure 1. Semilog plots of the power spectrum of the x, y, and z (vertical) components of the environmental magnetic noise. The magnetic field is measured in units of Tesla (T).

saddle coils, oriented in the vertical and horizontal directions. A sensor array was formed by fabricating a plastic holder with slots to accommodate multiple sensors, using a 3D printer. The holder had 12 slots, arranged in an offset square grid pattern of area 9×9 cm. The sensors were held in an inverted orientation so that the array could record from below a prone-lying subject. Only 10 sensors were available, so 2 slots in corners were left vacant. The holder was stationed on the patient table in a gap in the foam mattress (Figure 2). The height and orientation of the sensor array could be adjusted using shims and wedges to place it in contact with the abdomen of the mother. The sensors were oriented to record the components of the magnetic field transverse to the long axis of the cylindrical shield. This was done to reduce the contribution from environmental interference because the performance of cylindrical shields is significantly poorer in the longitudinal than the transverse direction. The patient table could slide on rails mounted to the inner surface of the cylindrical shield. A detachable extension with contiguous rails supported the patient table when it was outside the shield.

Two different magnetic shields were used: a standard 2-shell, mu-metal MSR (ETS-Lindgren, Inc, Glendale Heights, IL) and a 3-shell, mu-metal CS of inner diameter 0.75 m and length 2 m (Amuneal Inc, Philadelphia, PA). One end of the CS was capped, but the other was left open. The shield was mounted on a custom-made cart and could be easily transported. fMCG recordings were made using 3 sensor-shield configurations: SQUID sensors and MSR (SQUID-MSR); OPM sensors and cylindrical shield (OPM-CS); and OPM sensors and MSR (OPM-MSR). Whereas the main aim of the study was to compare the SQUID-MSR and OPM-CS configurations, we also made recordings on supine-lying subjects using the OPM-MSR configuration in order to demonstrate the increase in signal amplitude attributed to prone positioning. The sensor holder used for the OPM-MSR measurements was similar to the one described above for the OPM-CS measurements, but it suspended the sensors above the maternal surface in a noninverted orientation.[8]

Data Collection

The mother changed into nonmagnetic clothing. The SQUID-MSR data were recorded first. The mother lay on the patient table supine or on her side if she was uncomfortable lying supine. A brief ultrasound exam was performed to locate the position of the fetal heart. The magnetometer was positioned on the mother's abdomen as close as possible to the fetal heart. Two 10-minute recordings were made on normal fetuses and at least four 10-minute recordings were made on at-risk fetuses, moving the probe at least once. The recording time was longer for the at-risk fetuses because the SQUID-MSR data from these subjects were used for clinical management. Next, the OPM-CS recordings were made in a nearby room. The mother lay prone with the sensor array in contact with her

Table. Subject Characteristics, Waveform Interval, and SNR Measurements for the SQUID-MSR and OPM-CS Data, and the Ratio of the SNRs for the SQUID-MSR and OPM-CS Data

Fetus	GA (weeks)	Referral Diagnosis	In-Lab Echo	fMCG Rhythm	Device	PR (ms)	QRS (ms)	QTc (ms)	RR (ms)	SNR	$\frac{SNR_{OPM}}{SNR_{SQID}}$
1	30-6/7	1:1 tachycardia	1:1 tachycardia	Sinus tachycardia	SQUID	78	43	469	352	47.38	0.83
					OPM	81	46	461	364	39.14	
2	21-5/7	Normal	Normal	Normal	SQUID	78	42	462	414	10.17	0.99
					OPM	75	49	479	422	10.03	
3	26-6/7	Bradycardia (AV block)	Bradycardia (AV block or blocked atrial bigeminy)	Blocked atrial bigeminy	SQUID	112	56	520	719	13.88	0.93
					OPM	115	58	573	738	12.87	
4	26-1/7	Tachycardia and ectopy, 2° and 3° AV block, hydrops	Ventricular tachycardia, atrial flutter with variable block, hydrops	LQTS, TdP, AV block, PVCs, atrial flutter	SQUID	115	52	850*	846	. . .	. . .
					OPM	115	58	800*	1024	. . .	
5	20-6/7	Bradycardia (AV block), SSA+	Sinus rhythm, negative for AV block	Blocked PACs, negative for AV block	SQUID	73	38	461	402	7.90	1.41
					OPM	69	47	451	410	11.10	
6	24-0/7	2° and 3° AV block, SSA+	2:1 AV block with Wenckebach	2° AV block, ventricular tachycardia	SQUID	210	53	561	424	33.00	0.92
					OPM	217	54	528	422	30.45	
7	29-4/7	Obstetrical high risk; maternal ulcerative colitis	AV prolongation	Normal	SQUID	96	45	476	405	11.25	1.04
					OPM	96	43	474	401	11.66	
8	27-2/7	Normal	Normal	Normal	SQUID	89	35	408	403	6.63	0.87
					OPM	92	45	371	412	5.75	
9	31-2/7	Normal	Normal	Normal	SQUID	120	45	465	428	29.93	1.50
					OPM	124	49	450	432	44.88	
10	29-6/7	Bradycardia (AV block), ectopy	Bradycardia	Blocked atrial bigeminy, ectopy	SQUID	115	37	566	701	8.55	1.19
					OPM	113	40	562	670	10.15	
11	30-5/7	Obstetrical high risk	Normal	Normal	SQUID	106	37	475	421	6.38	3.84
					OPM	114	42	480	420	24.51	
12	31-4/7	Bradycardia (AV block)	Normal	Normal, negative for AV block	SQUID	112	54	414	444	10.30	1.16
					OPM	118	54	405	452	11.94	
13	24-6/7	Normal	Normal	Normal	SQUID	109	35	366	427	37.38	0.88
					OPM	114	41	362	422	32.99	
14	33-3/7	Normal	Normal	Normal	SQUID	109	37	393	448	9.60	2.19
					OPM	106	43	405	418	21.02	
15	21-2/7	Normal	Normal	Normal	SQUID	100	37	372	406	9.87	1.49
					OPM	99	40	367	410	14.66	
16	27-0/7	Maternal LQTS	Normal	Normal, negative for LQTS	SQUID	100	43	447	447	14.18	1.63
					OPM	109	46	441	460	23.11	
17	21-0/7	Bradycardia (AV block)	Normal	Normal, negative for AV block	SQUID	64	38	430	431	13.02	0.67
					OPM	68	36	435	447	8.73	
18	29-5/7	Maternal LQTS	Sinus rhythm	LQTS, T-wave alternans	SQUID	89	40	582	491	13.70	1.36
					OPM	83	38	612	511	18.58	
19	34-6/7	Maternal LQTS, AV block	Sinus bradycardia	LQTS, rare 2° AV block	SQUID	79	43	550	551	20.75	0.91
					OPM	74	46	559	558	18.79	
20	24-1/7	1:1 Tachycardia	1:1 Tachycardia	Sinus tachycardia	SQUID	106	45	317	305	8.30	1.52

Continued

Table. Continued

Fetus	GA (weeks)	Referral Diagnosis	In-Lab Echo	fMCG Rhythm	Device	PR (ms)	QRS (ms)	QTc (ms)	RR (ms)	SNR	$\frac{SNR_{OPM}}{SNR_{SQID}}$
					OPM	113	49	316	317	12.65	
21	32-0/7	1:1 Tachycardia	1:1 Tachycardia	Atrial ectopic tachycardia	SQUID	100	38	392	385	8.99	2.79
					OPM	103	42	413	364	25.08	
22	34-2/7	Sinus bradycardia	Sinus bradycardia	LQTS	SQUID	113	45	541	584	13.73	1.01
					OPM	109	46	572	597	13.94	
23	22-2/7	Maternal LQTS	Normal	Normal, negative for LQTS	SQUID	94	43	446	420	9.76	0.68
					OPM	96	41	446	462	6.67	
24	20-3/7	Ectopy and AV block	Ectopy	Ectopy, negative for AV block	SQUID	109	42	351	452	9.95	1.42
					OPM	113	40	380	450	14.12	

Fetus #4 showed rare sinus beats. The waveform intervals were measured from rhythm strips, but the QT measurements for this subject (asterisk) were not corrected for heart rate. AV indicates atrioventricular; fMCG, fetal magnetocardiography; GA, gestational age; LQTS, long QT syndrome; OPM-CS, Optically Pumped Magnetometer/Cylindrical Shield; PAC, premature atrial contractions; PVC, premature ventricular contraction; SNR, Signal-to-Noise Ratio; SQUID-MSR, Superconducting Quantum Interference Device/Magnetically Shielded Room; SSA, Sjogren's syndrome A; TdP, torsades de pointes.

abdomen from below. At least two 5-minute recordings were made, moving the sensor position at least once. Last, the OPM-MSR recordings were made. This required disassembling, transporting, and redeploying the OPM sensors and data acquisition system from the CS to the MSR. For this measurement, the mother lay supine or slightly on 1 side. At least two 5-minute recordings were made, moving the sensor position at least once. In 2 subjects, the OPM-MSR recordings were not made because of time constraints.

An in-lab echocardiogram was performed by a board-certified fetal cardiologist to assess fetal rhythm and allow comparison with the fMCG findings.

Statistical Analysis

The performance of the systems was compared by computing the SNR. Signal processing was applied to band-limit the raw recording to 1 to 80 Hz and remove maternal magnetocardiography interference.[9] A minimum mean squared error spatial filter[10] was applied to attenuate environmental and other interferences. The SNR was defined as the peak-to-peak amplitude of the fetal QRS complex divided by the root-mean-square amplitude of the noise, where the noise was estimated during the silent period of the cardiac cycle from the end of the T-wave to the beginning of the P wave of the following cycle. A binary test was used to compare the SNRs of the OPM-CS and SQUID-MSR configurations, and the signal amplitudes of the OPM-CS and OPM-MSR configurations. $P<0.05$ were considered significant.

Waveform interval measurements were made on averaged waveforms. Approximately 50 consecutive complexes were averaged during periods of fetal quiescence when the heart rate was relatively constant and near baseline, using autocorrelation to time align the complexes. Waveform intervals were measured from "butterfly" plots of the averaged waveforms, which superimpose all the channels. We measured the PR, QRS, QT, and RR intervals. QTc was computed using Bazett's formula: $QTc=QT/RR^{1/2}$. Concordance between the OPM-CS and SQUID-MSR measurements was evaluated by computing the concordance correlation coefficient.[11] Coefficients >0.95 were considered to indicate high concordance. A MATLAB (The MathWorks, Inc, Natick, MA) program was used to compute the concordance correlation coefficient and perform the binary test.

Results

In 1 fetus (#4), it was not possible to perform waveform averaging or measure the noise to compute the SNR because the rhythm was so complex and irregular that we could not reliably identify periods devoid of signal.

The SNR was greater for the OPM-CS data in 14 of 23 subjects ($P=0.097$) and, on average, was greater by a factor of 1.35 (Table); however, the difference was not statistically significant. The fact that the SNR was similar for the 2 systems was somewhat surprising, because the interference was visibly higher for the OPM-CS system because of the open-ended shield. The increased interference, however, was compensated by an increase in signal amplitude attributed to prone positioning, as could be observed from comparison of the signal amplitudes of the OPM-CS and OPM-MSR data, which used the same sensors but different positioning. Signal amplitude was greater for the OPM-CS data in 18 of 22 subjects ($P=0.002$) and, on average, was greater by a factor of 2.63. Signal amplitudes of the OPM-CS and SQUID-MSR data are not directly comparable because the OPMs measure the

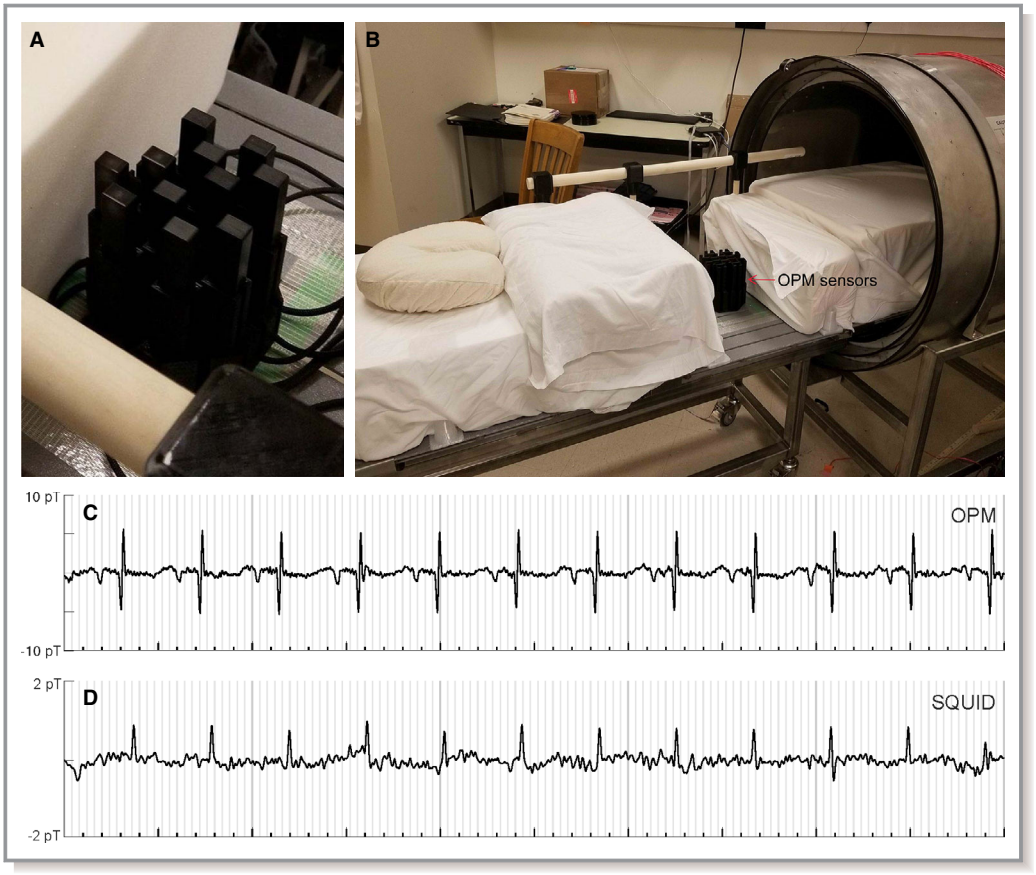

Figure 2. **A**, Photograph of 3D-printed inverted sensor holder populated with 11 optically pumped magnetometer (OPM) sensors. **B**, Photograph showing the open end of the cylindrical shield, the sliding patient table, and the OPM sensors. **C**, OPM recording in cylindrical shield with subject lying prone. **D**, Superconducting Quantum Interference Device (SQUID) recording in MSR from same subject as in **(C)** with subject lying on her side. The rhythm strips are 5 seconds in duration. The gray vertical lines are 40 ms apart. MSR indicates magnetically shielded room.

magnetic field and the SQUIDs measure the magnetic field gradient; thus, the SQUIDs register weaker signal, as well as weaker interference, because they measure magnetic field differences.

Figure 3C and 3D shows OPM and SQUID recordings taken from fetus #11 at 30-5/7 weeks and depicts an important advantage of prone positioning. The mother was unable to lie supine because of back pain, so the SQUID recordings were made with the mother lying on her side. As is typical in this circumstance, the signal was relatively weak because the SQUID sensor could not be optimally positioned and angled because of its bulkiness. Two other subjects could lie supine for approximately 10 minutes and then lay partly on their side for the remainder of the study. Prone positioning not only increased the signal amplitude of the OPM data, but it also improved patient comfort. All subjects reported that prone positioning was as comfortable as, or more comfortable than, supine positioning.

Table shows the referral diagnosis based on echocardiography, the in-lab echocardiogram findings, and the fMCG findings, including waveform intervals and SNR. The fMCG findings were consistent for the SQUID and OPM data. They were also compatible with the in-lab echocardiography findings, except for 1 fetus (#7), in which the mechanical PR was markedly prolonged (190–220 ms), but the magnetic PR was normal (96 ms). Importantly, fMCG provided additional information in several fetuses, most notably the fetuses with LQTS (#4, #18, #19, and #22). Figures 3 and 4 show tracings from the OPM-CS and SQUID-MSR systems. Although the main intent is to allow comparison of the technical performance of the 2 systems, the data were taken from the fetuses with clinically significant arrhythmias and provide an indication of the diagnostic information contained in fMCG recordings. Figure 3A through 3F shows averaged waveforms from three (#18, #19, and #22) of 4 fetuses that showed marked QTc prolongation. Except in Figure 3F, the waveforms

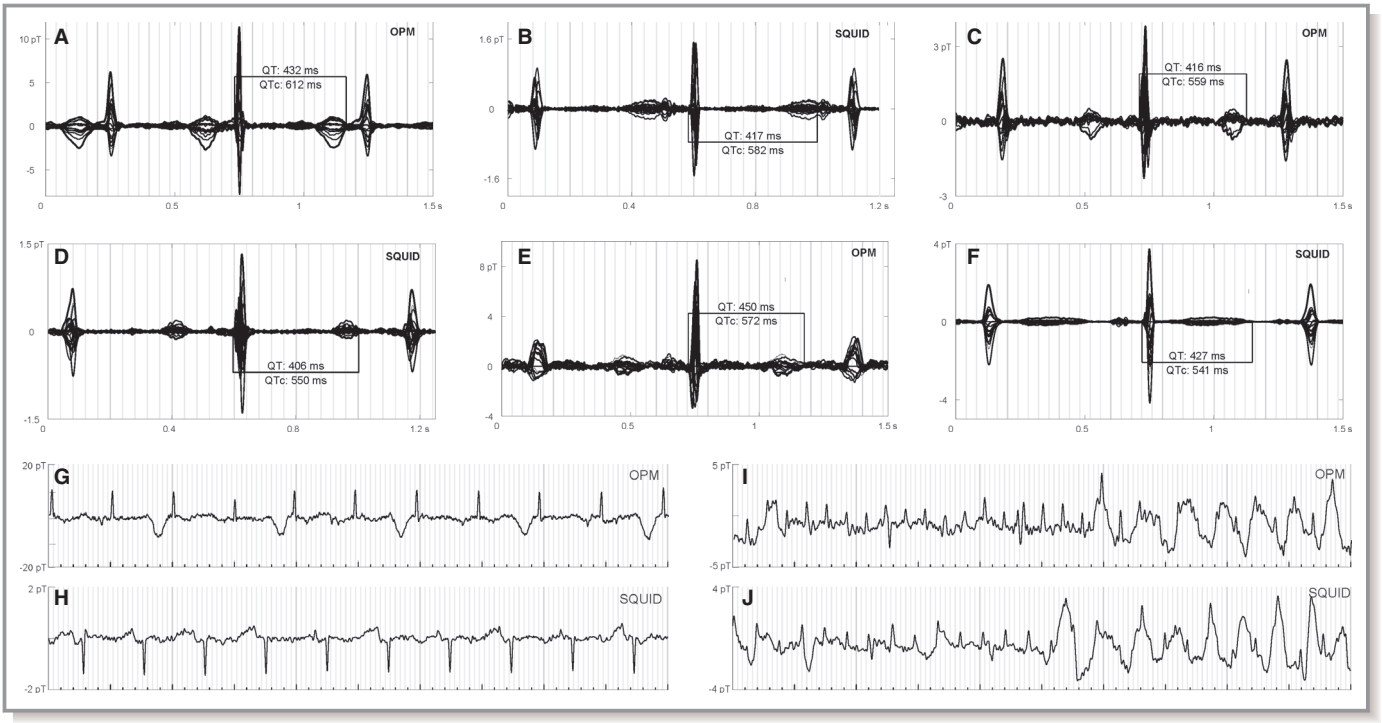

Figure 3. Long QT syndrome waveforms and rhythms. Fetuses #18 **(A** and **B)**, #19 **(C** and **D)**, and #22 **(E** and **F)** showed QTc prolongation. In **(B)**, the QTc is likely longer than shown; however, the T-wave termination is obscure because of overlap with the P wave. Fetus #18 showed prominent T-wave alternans **(G** and **H)**. Fetus #4 showed complex rhythms, including atrial flutter and torsade des pointes **(I** and **J)**. The rhythm strips are 5 seconds in duration. The gray vertical lines are 40 ms apart. OPM indicates optically pumped magnetometer; SQUID, Superconducting Quantum Interference Device.

show late-peaking T-waves, a distinctive marker of LQTS in the fetus. Whereas waveform averaging increases the SNR and allows weak components to be resolved, the true quality of the data is best surmised from inspection of the raw tracings, which allows assessment of irregular rhythms and episodic phenomena. Fetus #18, for example, showed prominent T-wave alternans (Figure 3G), a critical indicator of cardiac instability that is very rare postnatally. The fourth fetus with marked QTc prolongation (#4) was referred because of an extremely complex rhythm showing atrial and ventricular ectopy and tachycardia, and second- and third-degree atrioventricular (AV) block. The fMCG of this fetus was dominated by episodes of torsades de pointes, alternating with a highly irregular rhythm characterized by AV block, frequent premature ventricular contractions, and relatively rare sinus beats with marked QTc prolongation. In addition, periods of atrial flutter were observed (Figure 3I). To our knowledge, atrial flutter has not been previously reported in association with fetal LQTS.

Examples of sustained tachycardia or bradycardia are shown in Figure 4. Fetus #21 was referred with a diagnosis of tachycardia, but the form of tachycardia was uncertain. The heart rate was wide-ranging (130–240 bpm with mean 170 bpm), and it was thought that the periods of higher rate were possibly attributed to junctional or ventricular tachycardia. Despite the changes in heart rate, the fMCG showed that the rhythm was unchanged throughout and that the tachycardia was incessant atrial tachycardia (Figure 4A and 4B). The morphology of the P wave was compatible with a focus in the right atrial appendage.[12] Two other fetuses (#1 and #20) were found to have sinus or atrial ectopic tachycardia. Fetus #3 was referred with bradycardia thought to be second-degree AV block. The fMCG showed that the bradycardia was attributed to blocked atrial bigeminy (Figure 4C and 4D). Fetus #10 was also found to have blocked atrial bigeminy. Fetus #6 was referred with AV block, which was predominantly second degree, but on occasion appeared to be third-degree. The fMCG showed second-degree AV block with paroxysms of ventricular tachycardia, which had not been noted by ultrasound (Figure 4E and 4F).

Normal fMCGs were observed in 6 normal fetuses, 2 fetuses with high-risk obstetrical conditions, 2 fetuses with a family history of LQTS, 2 Sjogren's syndrome A–negative fetuses referred with sustained bradycardia thought to be second-degree AV block, and 2 Sjogren's syndrome A–positive fetuses referred with episodic bradycardia. The fMCG of the latter 2 fetuses, studied at 20-1/7 and 20-6/7 weeks, showed ectopy and occasional V-shaped decelerations, which are common and normal at that time.

Figure 4. Comparison of optically pumped magnetometer (OPM) and Superconducting Quantum Interference Device (SQUID) rhythm strips in fetuses with tachycardia and bradycardia. Fetus #21 **(A** and **B)** showed atrial ectopic tachycardia. Fetus #3 **(C** and **D)** showed bradycardia and ectopy because of blocked atrial bigeminy. Fetus #6 **(E** and **F)** showed second-degree AV block with brief episodes of ventricular tachycardia. P waves (asterisks) often show low SNR in the raw tracings. The rhythm strips are 5 seconds in duration. The gray vertical lines are 40 ms apart. AV indicates atrioventricular; SNR, signal-to-noise ratio.

The concordance correlation coefficients were 0.98 for PR, 0.74 for QRS, 0.97 for QTc, and 0.95 for RR. Comparisons of the PR, QRS, QTc, and SNR data are shown graphically in Figure 5.

Discussion

In this study, we demonstrated, for the first time, an fMCG system that combined OPM sensors with a person-sized magnetic shield. Remarkably, the system performed as well as a SQUID-based system at a small fraction of the cost. OPMs are much more cost-effective than SQUIDs for fMCG and other low channel-count applications because they do not require liquid helium and the associated cryogenics. Their small size enables the use of person-sized shields, which cost far less than MSRs and allows the entire system to be portable.

From a technical standpoint, the most challenging aspect of the study was the use of an open-ended magnetic shield. Open-ended shields have been used previously for magnetoencephalography.[13,14] In those studies, however, subjects entered the shield head first so that the sensors were situated near the closed end, where the shielding performance is

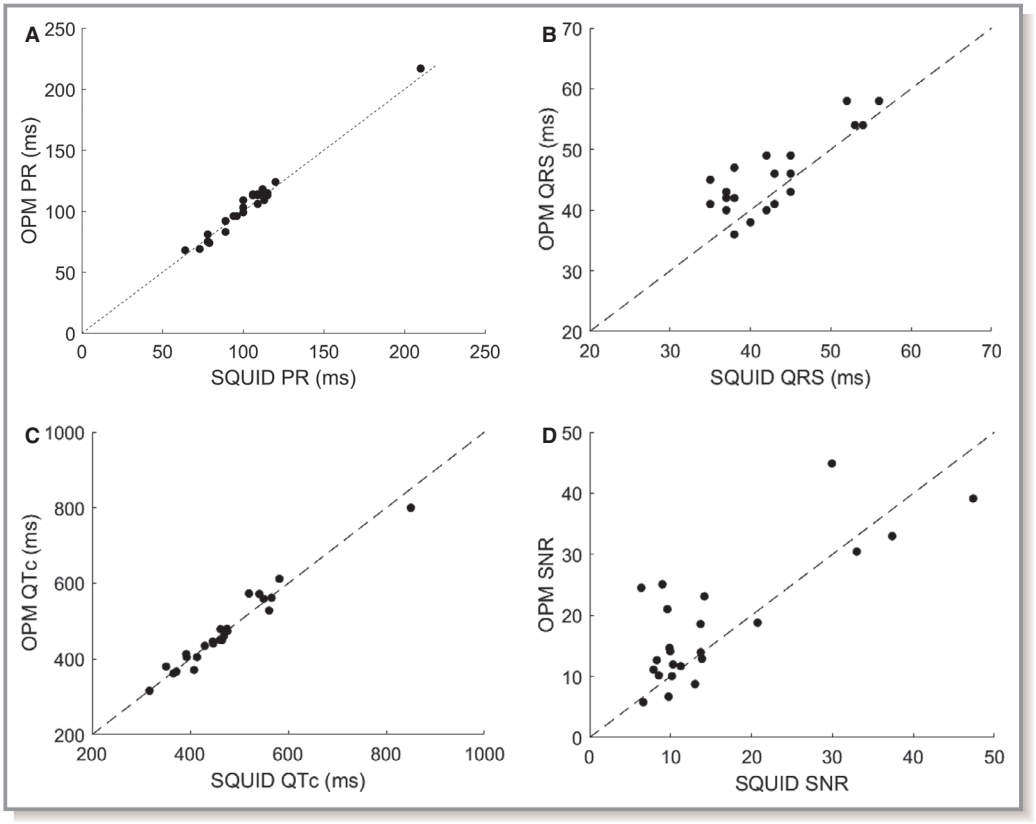

Figure 5. Optically pumped magnetometer (OPM) vs Superconducting Quantum Interference Device (SQUID) scatter plot comparisons of **(A)** PR, **(B)** QRS, **(C)** QTc, and **(D)** signal-to-noise ratio (SNR).

highest. The shields used in those studies were also greater in length and diameter, which allows accommodation of larger patients but increases cost. In our setup, mothers entered the shield feet first so that their heads were only approximately 0.3 m from the opening. This alleviated anxiety and greatly reduced the possibility of claustrophobia. The sensors, however, were located near the middle of the shield, where the shielding performance is significantly poorer than it is near the closed end. Despite the resulting increase in environmental noise, the SNR for the OPM-CS system was not degraded in comparison with the SQUID-MSR. This was possible mainly because the increase in environmental noise was compensated by an increase in signal amplitude attributed to prone positioning, which allowed the fetal heart to drop close to the sensors. An added benefit was that the mother was more comfortable when lying prone, versus supine, and this reduced movement artifact. In addition, the increased environmental interference was mitigated by orienting the sensors to measure only the components of the signal transverse to the long axis of the cylinder. These components show higher SNR because the shielding factor of a cylindrical shield is nearly a factor of 10 higher in the transverse than the longitudinal direction. Restricting the measurement to the transverse signal components does not appreciably compromise signal detection because signal amplitude is typically strongest for the component normal to the maternal surface, which is predominantly vertical. The SNR can be further increased by implementing modest improvements to the shielding or other noise reduction techniques, which we plan to do in future studies.

In addition to SNR, waveform interval measurements were used to compare data from the OPM and SQUID systems. The measurements showed good agreement, except for QRS. The imprecision of determining onset and termination of the waveform components is likely similar for all the components, but the percent uncertainty is higher for QRS given that it is the shortest interval. For clinical application, however, the ultimate measure of success is the ability of the cardiologist to assess rhythm and make an accurate diagnosis. The excellent performance of the OPM, as well as the SQUID, system was corroborated by the efficacy of the data for evaluation of fetuses with serious arrhythmia. The most notable examples were fetuses at risk of LQTS. fMCG was invaluable in these cases for its ability to diagnose QTc prolongation and ominous rhythms, such as T-wave alternans and torsade des pointes, which are difficult or impossible to diagnose with echocardiography. For fetuses with sustained tachycardia or bradycardia, the waveform information

provided by fMCG, along with the ability to continuously monitor rhythm and rate for extended periods, allows for a more-precise and/or definitive differential diagnosis than was possible with fetal echocardiography alone.

Currently, there are no commercial vendors of turn-key, OPM-based fMCG systems. A major advantage of OPM technology, however, is simplicity that enables an end user to assemble an investigational system, as was demonstrated here. The 2 main components of the system, the sensors and shield, can be purchased for as little as $100 000, and the remaining components can be procured at modest cost. Further details and assistance can be obtained by contacting the corresponding author. The ability to deploy OPM sensors for multiple applications is another important advantage that increases the cost-effectiveness of OPMs. In particular, the shield and sensors used in this study can be easily reconfigured to form a similarly low-cost adult magnetocardiography system. In contrast, our SQUID-MSR system costs ≈$1M, requires continual replenishment of liquid helium, and cannot be reconfigured for other applications.

In conclusion, we have demonstrated an fMCG system based on a new magnetometer technology that represents a major leap forward in practicality and cost-effectiveness. This advance has the potential to greatly increase the utilization of fMCG and enable routine assessment of the cardiac electrophysiology of the fetus.

Sources of Funding

This work was supported by the National Institutes of Health (Bethesda, MD) grant numbers R21 EB025901, R01 HL63174, and R44 HL114182. Oswaldo Baffa's participation in the research was supported by a Fulbright Scholarship. The study was supported, in part, by a Small Business Innovative Research grant (R44 HL114182) awarded to QuSpin, Inc. The funding organizations had no role in any of the following: design and conduct of the study; collection, analysis, and interpretation of the data; or the preparation, review, and approval of the manuscript.

Disclosures

Wakai, PhD, is the principal investigator of the NIH grants R21 EB025901 and R01 HL63174. This disclosure is modest. Vishal Shah, PhD, is the founder and Chief Scientist of QuSpin, Inc. This disclosure is significant. Shah is the principal investigator of the NIH grant R44 HL114182. This disclosure is modest. The remaining authors have no disclosures to report.

References

1. Cuneo BF, Strasburger JF, Yu SH, Horigome H, Hosono T, Kandori A, Wakai RT. In utero diagnosis of long QT syndrome by magnetocardiography. *Circulation*. 2013;128:2183–2191.
2. Zhao H, Cuneo BF, Strasburger JF, Huhta JC, Gotteiner NL, Wakai RT. Electrophysiological characteristics of fetal atrioventricular block. *J Am Coll Cardiol*. 2008;51:77–84.
3. Strasburger JF, Wakai RT. Fetal cardiac arrhythmia detection and in utero therapy. *Nat Rev Cardiol*. 2010;7:277–290.
4. Wiggins DL, Strasburger JF, Gotteiner NL, Cuneo B, Wakai RT. Magnetophysiologic and echocardiographic comparison of blocked atrial bigeminy and 2:1 atrioventricular block in the fetus. *Heart Rhythm*. 2013;10:1192–1198.
5. Donofrio MT, Moon-Grady AJ, Hornberger LK, Copel JA, Sklansky MS, Abuhamad A, Cuneo BF, Huhta JC, Jonas RA, Krishnan A, Lacey S, Lee W, Michelfelder EC Sr, Rempel GR, Silverman NH, Spray TL, Strasburger JF, Tworetzky W, Rychik J; American Heart Association Adults With Congenital Heart Disease Joint Committee of the Council on Cardiovascular Disease in the Young and Council on Clinical Cardiology, Council on Cardiovascular Surgery and Anesthesia, and Council on Cardiovascular and Stroke Nursing. Diagnosis and treatment of fetal cardiac disease: a scientific statement from the American Heart Association. *Circulation*. 2014;129:2183–2242.
6. Fagaly RL. Neuromagnetic instrumentation. *Adv Neurol*. 1990;54:11–32.
7. Kominis IK, Kornack TW, Allred JC, Romalis MV. A subfemtotesla multichannel atomic magnetometer. *Nature*. 2003;422:596–599.
8. Batie M, Bitant S, Strasburger JF, Shah V, Alem O, Wakai RT. Detection of fetal arrhythmia using optically-pumped magnetometers. *JACC Clin Electrophysiol*. 2018;4:284–287.
9. Yu S, Wakai RT. Maternal MCG interference cancellation using splined independent component subtraction. *IEEE Trans Biomed Eng*. 2011;58:2835–2843.
10. Chen M, Van Veen BD, Wakai RT. Linear minimum mean-square error filtering for evoked responses: application to fetal MEG. *IEEE Trans Biomed Eng*. 2006;53:959–963.
11. Lin LI. A concordance correlation-coefficient to evaluate reproducibility. *Biometrics*. 1989;45:255–268.
12. Tang CW, Scheinman MM, Van Hare GF, Epstein LM, Fitzpatrick AP, Lee RJ, Lesh MD. Use of P wave configuration during atrial tachycardia to predict site of origin. *J Am Coll Cardiol*. 1995;26:1315–1324.
13. Xia H, Baranga ABA, Hoffman D, Romalis MV. Magnetoencephalography with an atomic magnetometer. *Appl Phys Lett*. 2006;89:211104-1-3.
14. Borna A, Carter TR, Goldberg JD, Colombo AP, Jau Y-Y, Berry C, McKay J, Stephen J, Weisend M, Schwindt PDD. A 20-channel magnetoencephalography system based on optically pumped magnetometers. *Phys Med Biol*. 2017;62:8909–8923.